

# Low Energy Wireless Body-Area Networks for Fetal ECG Telemonitoring via the Framework of Block Sparse Bayesian Learning

Zhilin Zhang, *Student Member, IEEE*, Tzyy-Ping Jung, *Senior Member, IEEE*  
Scott Makeig, Bhaskar D. Rao, *Fellow, IEEE*

**Abstract**—Fetal ECG (FECG) telemonitoring is an important branch in telemedicine. The design of a telemonitoring system via a low-power wireless body-area network for ambulatory use is highly desirable. As an emerging technique, compressed sensing (CS) shows great promise in compressing data with low power consumption. However, due to some specific characteristics of FECG recordings such as non-sparsity and strong noise contamination, current CS algorithms generally fail in this application.

In this work we utilize the block sparse Bayesian learning (bSBL) framework, a recently developed framework solving the CS problems. To illustrate the ability of the bSBL methods, we apply it to two representative FECG datasets. In one dataset the fetal heartbeat signals are visible, while in the other dataset are barely visible. The experiment results show that the bSBL framework is capable of compressing FECG raw recordings and successfully reconstructing them. These successes rely on two unique features of the bSBL framework; one is the ability to reconstruct less-sparse but structured signals, and the other is the ability to learn and exploit correlation structure of signals to improve performance. These two abilities of the framework greatly enhance the potential use of bSBL in telemonitoring of other physiological signals.

**Index Terms**—Fetal ECG (FECG), Telemonitoring, Compressed Sensing (CS), Block Sparse Bayesian Learning (bSBL), Wireless Body-Area Network (WBAN), Telemedicine

## I. INTRODUCTION

Noninvasive monitoring of fetal electrocardiogram (FECG) is an important approach to monitoring fetus health state. The physiological parameters of FECG signals, such as heart beat rates, morphology, and dynamic behaviors, can be used for diagnosis of fetal development and disease. Among these parameters, the heart beat rate is the main index of fetal assessment for high-risk pregnancies [1]. For example, abnormal patterns (decelerations, loss of high-frequency variability, and pseudo-sinusoidal) of fetal heart beat rates are generally indicative of fetal asphyxia [2].

However, to noninvasively obtain clean FECG from maternal abdominal recordings is not an easy problem. The FECG signal itself is very weak. Since it is recorded from the mother's abdomen, it is embedded in strong noise and

interference, which include maternal ECG (MECG), instrumental noise, artifacts caused by muscle, uterine contractions and respiration. Further, the gestational age and the position of the fetus also affect the strength of FECG in abdominal recordings. Up to now various signal processing and machine learning methods have been proposed to obtain FECG, such as adaptive filtering [3], wavelet analysis [4], and blind source separation (BSS) or independent component analysis (ICA) [5]. Interested readers can refer to [4], [6], [2] for good surveys on these techniques.

Traditionally, pregnant women are required to frequently visit hospitals to get resting FECG monitoring. Now, the trend and desire is to allow pregnant women to get ambulatory monitoring of FECG. For example, pregnant women can stay at home. This can be achieved by wireless telemonitoring. In such a telemonitoring system, a wireless body-area network (WBAN) [7] integrates a number of sensors attached on a patient's skin, and uses ultra-low-power short-haul radios (e.g. Bluetooth Low End Extension Radio) in conjunction with nearby smart-phones or handheld devices to communicate via the Internet with the health care provider in a remote terminal. Telemonitoring is a convenient way for patients to avoid frequent visiting to hospitals and save lots of time and medical cost.

Among many constraints in WBAN-based telemonitoring systems [8], the energy constraint is a primary design constraint [9], [10] since a WBAN is battery operated. It is necessary to reduce power consumption as much as possible. This has to be done in a constrained environment. One constraint is that on-sensor computation should be minimum. Another constraint is that data should be compressed before transmitting (the compressed data will be used to reconstruct the original data in remote terminals). Unfortunately, most conventional data compression techniques such as wavelet-based algorithms dissipate lots of energy [11]. So, new compression techniques are needed urgently.

Compressed sensing (CS) [12], [13], [14], an emerging signal processing technique, is a promising tool to cater to the two constraints. It uses a simple linear transform (i.e. a sensing matrix) to compress a signal, and then reconstructs the original signal by exploiting its sparsity. The sparsity refers to the characteristics that most entries of the signal are zero or near zero. When CS is used in WBAN-based telemonitoring systems, the compression stage is completed on data acquisition module before transmission, while the

Z.Zhang and B.D.Rao are with the Department of Electrical and Computer Engineering, University of California, San Diego, La Jolla, CA 92093-0407, USA. Email: {z4zhang, brao}@ucsd.edu

T.-P. Jung and S. Makeig are with the Swartz Center for Computational Neuroscience, University of California, San Diego, La Jolla, CA 92093-0559, USA. Email: {jung, scott}@scn.ucsd.edu

reconstruction stage is completed on workstations/computers at remote terminals. Based on a real-time ECG telemonitoring system, Mamaghanian et al. [11] showed that when using a sparse binary matrix as the sensing matrix, CS can greatly extend sensor lifetime and reduce energy consumption while achieving competitive compression ratio, compared to a wavelet-based compression method. They also pointed out that when the data collection and the compression are implemented together by analog devices before analog-to-digital converter (ADC), the energy consumption can be further reduced.

Although CS has achieved some successes in adult ECG telemonitoring [11], [15], it encounters difficulties in FECG telemonitoring. These difficulties essentially come from the conflict between more strict energy constraint in FECG telemonitoring systems and non-sparsity of raw FECG recordings.

The energy constraint is more strict in FECG telemonitoring systems due to the large number of sensors deployed. Generally, the number of sensors to receive raw FECG recordings ranges from 8 to 16, and sometimes extra sensors are needed to record maternal physiological signals (e.g. blood pressure, MEKG, temperature). The large number of sensors indicates large energy dissipated in on-sensor computation. Given limited energy, this restricts the systems to perform other on-sensor computation as little as possible. For CS algorithms, this means that they are required to directly compress raw FECG recordings with none or minimum pre-processing.

However, a problem is that raw FECG recordings are inherently non-sparse, which seriously deteriorates the reconstruction quality of CS algorithms. Raw FECG recordings differ from adult ECG recordings in that they are unavoidably contaminated by a number of strong noise and interference, as discussed previously. Most CS algorithms have difficulty in directly reconstructing such non-sparse signals. Although some strategies have been developed for non-sparse signals for general cases, the energy constraint prevents the use of these strategies.

This study proposes to use the block sparse Bayesian learning (bSBL) framework [16], [17] to address these challenges. The bSBL framework, as a new framework solving the CS problems, has some advantages to conventional CS frameworks. It provides large flexibility to exploit spatial [18], temporal [17], and dynamic structure [19] of signals. Algorithms derived using this framework have superior performance to most existing CS algorithms [20]. Here, we discuss two interesting properties of the bSBL framework. One is its ability to reconstruct non-sparse signals with high quality. The other is its ability to exploit unknown structure of signals for better reconstruction quality. It is these two properties that enable the bSBL framework to achieve successes in wireless FECG telemonitoring. To the best of our knowledge, there is no other CS algorithms/frameworks that can achieve the same level of success.

The rest of the paper is organized as follows. Section II introduces basic CS models and the bSBL framework. Section III shows experiment results on two typical FECG datasets. Section IV discusses some issues related to the bSBL framework and our experiments. Discussions and conclusions are given in the last two sections.

## II. COMPRESSED SENSING (CS) AND BLOCK SPARSE BAYESIAN LEARNING (BSBL)

As in the ‘digital CS’ paradigm in [11], we assume signals have passed through the analog-to-digital converter (ADC).

### A. Compressed Sensing and Associated Models

Compressed sensing is a new data compression paradigm which relies on the sparsity of the signal to compress and reconstruct. The *basic noisy model* can be expressed as

$$\mathbf{y} = \Phi \mathbf{x} + \mathbf{v}, \quad (1)$$

where  $\mathbf{x} \in \mathbb{R}^{N \times 1}$  is the signal to compress/reconstruct with length  $N$ .  $\Phi \in \mathbb{R}^{M \times N}$  ( $M \ll N$ ) is a designed sensing matrix which linearly compresses  $\mathbf{x}$ .  $\mathbf{v}$  is a noise vector modeling errors incurred during this compression procedure or noise in the CS system. In the context of the task considered in this paper,  $\mathbf{x}$  is a segment from a raw FECG recording, and  $\mathbf{y}$  is the compressed data which will be transmitted via WBANs to remote terminals.

In remote terminals, using the designed sensing matrix  $\Phi$ , CS algorithms reconstruct  $\mathbf{x}$  from the compressed data  $\mathbf{y}$ . Note that reconstructing  $\mathbf{x}$  is an underdetermined inverse problem. By exploiting the sparsity of  $\mathbf{x}$  it is possible to recover it with small errors in noisy environment [14].

In many applications the signal  $\mathbf{x}$  is not sparse, but sparse in some transformed domains such as the wavelet domain, i.e.  $\mathbf{x} = \Psi \boldsymbol{\theta}$ , where  $\Psi \in \mathbb{R}^{N \times N}$  is an orthonormal basis matrix of the transformed domain and  $\boldsymbol{\theta}$  is the coefficient vector representing  $\mathbf{x}$  in the transformed domain. Thus the basic noisy model (1) becomes

$$\mathbf{y} = \Phi \Psi \boldsymbol{\theta} + \mathbf{v} = \Omega \boldsymbol{\theta} + \mathbf{v}, \quad (2)$$

where  $\Omega \triangleq \Phi \Psi$ . Since  $\boldsymbol{\theta}$  is sparse, CS algorithms can first reconstruct  $\boldsymbol{\theta}$  using  $\mathbf{y}$  and  $\Omega$ , and then reconstruct  $\mathbf{x}$  by  $\mathbf{x} = \Psi \boldsymbol{\theta}$ . This method is useful for some kinds of signals. But as shown in our experiments later, this method still cannot help existing CS algorithms to reconstruct the original raw FECG recordings.

Sometimes the noise vector  $\mathbf{v}$  can be ignored, but the signal  $\mathbf{x}$  itself contains noise (called ‘*signal noise*’). That is,  $\mathbf{x} = \mathbf{u} + \mathbf{n}$ , where  $\mathbf{u}$  is the clean signal and  $\mathbf{n}$  is the signal noise. So the model (1) becomes

$$\mathbf{y} = \Phi \mathbf{x} = \Phi(\mathbf{u} + \mathbf{n}) = \Phi \mathbf{u} + \Phi \mathbf{n} = \Phi \mathbf{u} + \mathbf{w}, \quad (3)$$

where  $\mathbf{w} \triangleq \Phi \mathbf{n}$  is a new noise vector. This model is also called a ‘*noise-folding model*’ [21], and can be viewed as a basic noisy CS model.

Most natural signals have rich structure. It is shown that exploiting the structure can improve performance (e.g. reducing reconstruction errors, increasing compression ratio, etc) [22]. A widely studied structure is the block structure [23]. A sparse signal with this structure can be viewed as concatenation of  $g$  blocks, i.e

$$\mathbf{x} = \underbrace{[x_1, \dots, x_{d_1}]}_{\mathbf{x}_1^T}, \dots, \underbrace{[x_{d_{g-1}+1}, \dots, x_{d_g}]}_{\mathbf{x}_g^T}^T \quad (4)$$

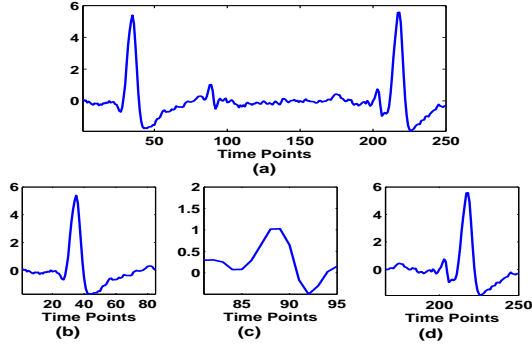


Fig. 1. Close-up of the second channel recording in the dataset shown in Fig. 2. (a) A segment of the first 250 time points of the recording. (b) A sub-segment containing a QRS complex of MECG. (c) A sub-segment containing a QRS complex of FECG. (d) A sub-segment showing a QRS complex of FECG contaminated by a QRS complex of MECG.

where  $\mathbf{x}_i \in \mathbb{R}^{d_i \times 1}$ , and  $d_i (i = 1, \dots, g)$  are not necessarily the same. Among the  $g$  blocks, only few blocks are nonzero. A signal with this block structure is called a *block-sparse signal*, and the model (1) with the block partition (4) is called a *block-sparse model*. It is known that exploiting such block structure can further improve recovery performance [22], [23].

A raw FECG recording can be roughly viewed as a block-sparse signal contaminated by signal noise. Figure 1 (a) plots a segment of a raw FECG recording. In this segment the parts from 20 to 60, from 85 to 95, and from 200 to 250 time points can be viewed as three significant nonzero blocks, while other parts can be viewed as concatenation of a number of zero blocks. Although entries in these ‘zero blocks’ are not strictly zero, these nonzero entries can be viewed as signal noise. But note that in FECG telemonitoring, the block partition of FECG recordings is unknown. Hence, raw FECG recordings can be modeled as a block-sparse model with unknown block partition and unknown signal noise in a noiseless environment.

Reconstructing  $\mathbf{x}$  while exploiting its unknown block partition is very difficult. Up to now only several CS algorithms have been proposed for this purpose. Huang et al [24] proposed a greedy algorithm called StructOMP, which is based on the coding complexity of the signal to reconstruct. Yu et al [25] proposed a Bayesian CS algorithm called CluSS-MCMC, in which a hierarchical Bayesian model is used to model both the sparse prior and block prior. Faktor et al [26] proposed a Bayesian algorithm, called BM-MAP-OMP, which models the sparsity structure by a Boltzmann machine.

Recently we proposed the framework of block sparse Bayesian learning (bSBL) [16], [17], and derived a family of algorithms [16]. Their abilities to reconstruct less-sparse signals and structured signals with unknown block partition endow them with superior performance to existing algorithms. In the following we will briefly introduce it. Interested readers can refer to [16], [17], [27], [28] for details.

### B. Block Sparse Bayesian Learning (bSBL)

For a block-sparse signal  $\mathbf{x}$  of the form (4), the bSBL framework models each block  $\mathbf{x}_i \in \mathbb{R}^{d_i \times 1}$  as a parameterized

multivariate Gaussian distribution:

$$p(\mathbf{x}_i) \sim \mathcal{N}(\mathbf{0}, \gamma_i \mathbf{B}_i), \quad i = 1, \dots, g \quad (5)$$

where  $\gamma_i$  is a nonnegative parameter controlling the block-sparsity of  $\mathbf{x}$ , and  $\mathbf{B}_i \in \mathbb{R}^{d_i \times d_i}$  is a positive definite matrix capturing the correlation structure of the  $i$ -th block. When  $\gamma_i = 0$ , the corresponding  $i$ -th block, i.e.  $\mathbf{x}_i$ , becomes a zero block. Based on the assumption (5), the prior of  $\mathbf{x}$  is  $p(\mathbf{x}) \sim \mathcal{N}(\mathbf{0}, \Sigma_0)$ , where  $\Sigma_0$  is a block-diagonal matrix with each principal block given by  $\gamma_i \mathbf{B}_i$ . The noise vector is assumed to satisfy a multivariate Gaussian distribution, namely  $p(\mathbf{v}) \sim \mathcal{N}(\mathbf{0}, \lambda \mathbf{I})$ , where  $\lambda$  is a positive scalar and  $\mathbf{I}$  is the identity matrix.

Based on this probabilistic model, three iterative algorithms [16], [18] have been derived to reconstruct  $\mathbf{x}$ . We choose the Bound-Optimization based Block SBL algorithm, denoted by BSBL-BO, for FECG telemonitoring since it has a good balance between speed and reconstruction performance. Its ability to reconstruct less-sparse signals is achieved by setting a  $\gamma_i$ -pruning threshold<sup>1</sup> to a small value. The threshold is used to prune out small  $\gamma_i$  during iterations of the algorithm (note that pruning out a  $\gamma_i$  is equivalent to setting the corresponding block in  $\mathbf{x}$ , i.e.  $\mathbf{x}_i$ , to a zero block). A smaller value of the threshold means fewer  $\gamma_i$  are pruned out, and thus fewer blocks in  $\mathbf{x}$  are forced to zero blocks. Consequently, the eventually estimated  $\mathbf{x}$  is less sparse. In our experiments we set the threshold to 0, i.e. disabling the pruning mechanism.

BSBL-BO (and other algorithms derived in [16]) has another ability, namely estimating and exploiting the correlation structure among entries in each block  $\mathbf{x}_i$  (i.e. the intra-block correlation) through learning the matrix  $\mathbf{B}_i$ . Our experiments will show this ability can allow it to achieve better reconstruction performance than approaches that cannot or do not exploit the correlation structure.

Although BSBL-BO needs users to define the block partition (4), we have shown [16] that it is not needed to require the user-defined block partition to be the same as the true block partition. In the next two sections we will further confirm this.

## III. EXPERIMENTS

We carry out experiments using two datasets of raw FECG recordings. In the first dataset, the fetal heartbeat signals are nearly visible, while in the second dataset the fetal heartbeat signals are barely visible. Thus the two datasets provide a good diversity of recordings to verify the efficacy of our algorithm under various situations (e.g. different pregnancy weeks).

It is pointed out [11] that using sparse binary sensing matrices in CS algorithms can reduce energy consumption. So we adopt this suggestion and thus focus on the investigation of CS algorithms for compressing/reconstructing raw FECG recordings. In our experiments the sparse binary sensing matrix was of the size  $125 \times 250$  and only 15 entries in each column were 1s. The locations of nonzero entries in each column were randomly selected. For the BSBL-BO algorithm, we defined its block partition as the one in (4) with  $d_1 = \dots =$

<sup>1</sup>Such threshold is used in most SBL algorithms [28], not merely in the bSBL framework.

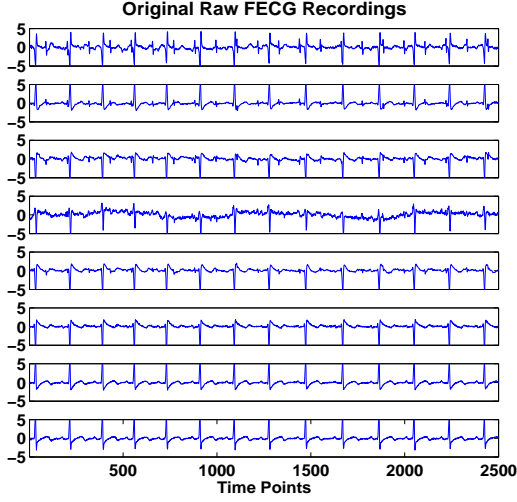


Fig. 2. The original raw FECG recordings. Each channel recording was normalized to have unit variance. This is often a routine step for BSS/ICA algorithms to extract clean FECGs, but not a requirement for CS algorithms to compress/reconstruct the recordings.

$d_g = d = 25$ . The choices of the sensing matrix size and the block partition were random. Section IV will show that the algorithm is not sensitive to the matrix size and the block partition.

For algorithm comparison, we chose eight important CS algorithms, each representing a family of algorithms and shown to have top-tier performance in its family. Thus the comparison results can be generalized to other related CS algorithms.

Since all CS algorithms used the same sparse binary matrix to compress FECG recordings, the energy consumption of each CS algorithm was the same (note that reconstruction of FECG recordings is done by software in remote terminals). Therefore we only present the reconstruction results.

In adult ECG telemonitoring or other applications, reconstruction performance is generally measured by comparing reconstructed recordings with original recordings using the mean square error (MSE) as a performance index. However, in our task reconstructing raw FECG recordings is not the final goal; the reconstructed recordings are further processed to extract a clean FECG using other advanced signal processing approaches (e.g. BSS/ICA). Due to the infidelity of the MSE for structured signals [29], it is hard to see how the final FECG extraction is affected by the reconstruction errors measured by MSE. Some reconstruction errors on MECG or other interference/noise may not significantly affect the quality of the final extracted FECG. So, a more direct measure is to compare the extracted FECG from the reconstructed FECG raw recordings with the extracted one from the original raw recordings. In our experiments we used BSS/ICA algorithms to extract a clean FECG from the reconstructed recordings and a clean FECG from the original recordings. And then calculate the correlation between the two extracted FECGs.

#### A. FECG Data 1: FECG is Nearly Visible

Figure 2 shows a set of real-world FECG recordings [30], which is widely studied in the FECG community. The recordings are sampled at 250 Hz. The first five channel recordings are obtained by sensors placed on the maternal abdomen, while the last three channel recordings are obtained by sensors placed on the maternal chest. The most obvious activity is the maternal cardiac activity (the heart rate is around 84 per minute), which can be seen in all the recordings. The fetal cardiac activity (the heart rate is around 132 per minute) is very weak, which is nearly discernible in the first five abdominal recordings. The fourth recording is dominated by a baseline wander caused by maternal respiration. Figure 1 gives a close-up view of the dataset. It is the segment of the first second of the second channel recording. In the segment two QRS complexes of MECG can be clearly seen, and two QRS complexes of FECG can be seen but not very clearly. Since MECG is much stronger than FECG, sometimes the QRS complexes of FECG are buried in the complexes of MECG, as shown in Fig.1 (d).

First, we use the segment in Fig.1 (a) as an example to discuss the difficulties for reconstruction and illustrate the performance of all algorithms. We can clearly see that the segment is far from sparse; its every entry is non-zero. This brings a huge difficulty for existing CS algorithms to reconstruct the segment. In adult ECG telemonitoring, some thresholding methods [31] are used to remove entries with near-zero amplitudes. However, the thresholding methods cannot be used for FECG recordings. The amplitudes of FECGs are very small and even invisible (see the second dataset in the next subsection), and the strength of FECGs depend on several uncertain factors such as pregnancy weeks and fetus position. It is difficult or even impossible to choose an optimal threshold value. Besides, if one chooses BSS/ICA to extract clean FECG from reconstructed recordings, these thresholding methods may destroy the underlying ICA mixing structure<sup>2</sup>, thus invalidating BSS/ICA algorithms. For the same reasons, some heartbeat detection methods [32] which work well for adult ECGs also cannot be applied to FECG recordings.

We used the sparse binary sensing matrix described before to compress the segment. For BSBL-BO, we employed it in two ways. The first way was allowing it to adaptively learn and exploit intra-block correlation. The second way was by preventing it from exploiting the intra-block correlation, i.e. by fixing the matrices  $\mathbf{B}_i(\forall)$  to identity matrices. The results are shown in Fig.3, from which we see that exploiting the intra-block correlation allows the algorithm to reconstruct the segment with high quality. If not exploiting the correlation structure, the reconstruction quality is very poor; for example, the first QRS complex of FECG is missed in the reconstructed segment (Fig.3 (c)).

Then we employed two groups of CS algorithms. One group are the algorithms based on the basic CS model (1), which do

<sup>2</sup>The problem of extracting clean FECGs from raw FECG recordings can be well modeled as an instantaneous ICA mixture model. In this model, the raw recordings are viewed as the linear mixture of a number of underlying sources including FECG components, MECG components, and various noise. Details can be found in [5], [6].

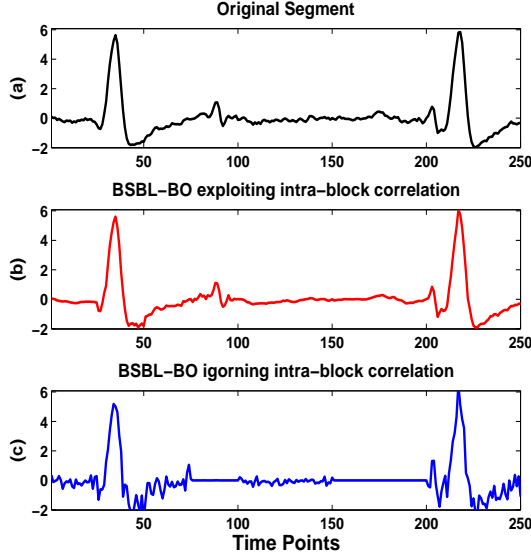


Fig. 3. Comparison of the original segment and the reconstructed segments by BSBL-BO with and without exploiting intra-block correlation. (a) The original FECG segment. (b) The reconstructed segment by BSBL-BO when exploiting intra-block correlation. (c) The reconstructed segment by BSBL-BO when not exploiting intra-block correlation.

not exploit block structure of signals. These algorithms are CoSaMP [33], Elastic-Net [34], SL0 [35], and EMBGAMP [36]. They are representative of greedy algorithms, of  $\ell_1/\ell_2$  mixed-norm based algorithms, of  $\ell_0$ -norm based algorithms, and of message passing algorithms, respectively. Their reconstructed results are shown in Fig.4. Clearly, all of them fail to reconstruct the segment <sup>3</sup>.

The second group are the algorithms estimating and exploiting structure of signals. They are the four algorithms mentioned in Section II-A, namely Block-OMP [23], CluSS-MCMC [25], StructOMP [24], and BM-MAP-OMP [26]. Block-OMP needs a priori knowledge of block partition. We used the block partition in (4) with  $d_1 = \dots = d_g = d$  and the block size  $d$  varied from 2 to 50. However, neither block size yielded meaningful results. Figure 5 (a) shows the result when the block size was set to 25. Figure 5 (b) shows the reconstruction result of CluSS-MCMC. StructOMP requires a priori knowledge of the sparsity (i.e. the number of nonzero entries in the segment). Since in the experiment we did not know the sparsity, we set the sparsity from 50 to 200. However, no sparsity value led to a useful result. Figure 5 (c) shows the result with the sparsity set to 120. Figure 5 (d) shows the result of BM-MAP-OMP. Clearly, all the four algorithms fail to reconstruct the segment.

Comparing all the results we can see only the BSBL-BO algorithm, if allowed to exploit intra-block correlation, can reconstruct the segment with satisfying quality. To further verify its ability, we used the same sensing matrix to compress the whole FECG recordings shown in Fig.2, and used BSBL-BO to reconstruct them. The results are shown in Fig.6. We can

<sup>3</sup>The free parameters of these algorithms were tuned by try and error. But no values were found to give meaningful results.

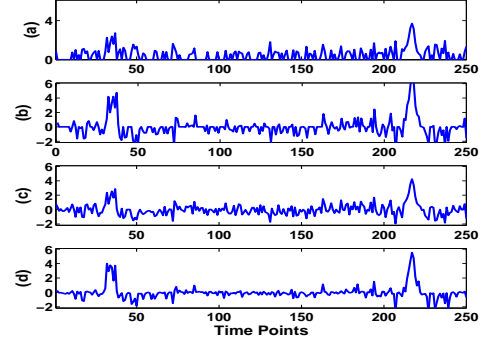


Fig. 4. Reconstruction results by (a) CoSaMP, (b) Elastic Net, (c) SL0, and (d) EMBGAMP, respectively.

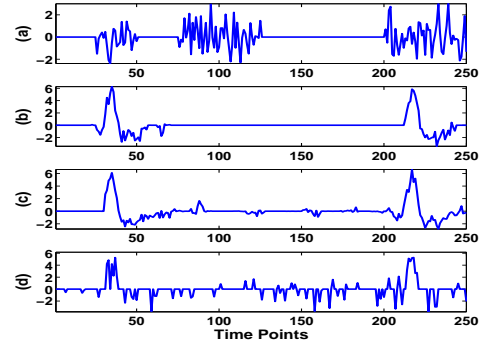


Fig. 5. Reconstruction results by Block-OMP (a), CluSS-MCMC (b), StructOMP (c), and BM-MAP-OMP (d), respectively.

see all the recordings are reconstructed very well. Visually, we do not observe any distortions in the reconstructed recordings.

But admittedly the reconstructed recordings contained small errors. Since in FECG telemonitoring the final goal is to extract a clean FECG from the reconstructed FECG recordings using advanced signal processing methods such as BSS/ICA, we examined whether these small errors deteriorated the performance of these advanced signal processing methods. Particularly we examined whether the errors affected the performance of BSS/ICA. We used the eigBSE algorithm, a BSS algorithm proposed in [37], to extract a clean FECG from the reconstructed recordings. The eigBSE algorithm exploits quasi-periodic characteristics of FECGs. Thus, if the quasi-periodic structure of FECGs and the ICA mixing structure of the recordings are distorted, the extracted FECGs will have poor quality.

The extraction result is shown in Fig.7 (a). We can see the FECG is clearly extracted without losing any QRS complexes or containing residual noise/interference. For a comparison, we performed the eigBSE algorithm to extract the FECG from the original recordings. The result is shown in Fig.7 (b). We can see the two extracted FECGs are almost the same. In fact, their correlation is 0.931. This result suggests that the BSBL-BO algorithm is very effective for FECG telemonitoring.



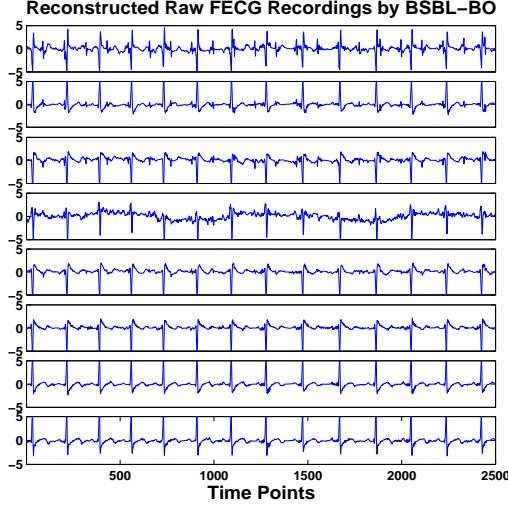


Fig. 6. The reconstructed recordings by BSBL-BO. Note that not only the weak fetal heartbeat signals but also other noise/interference such as the noise caused by respiration were maintained in the recordings.

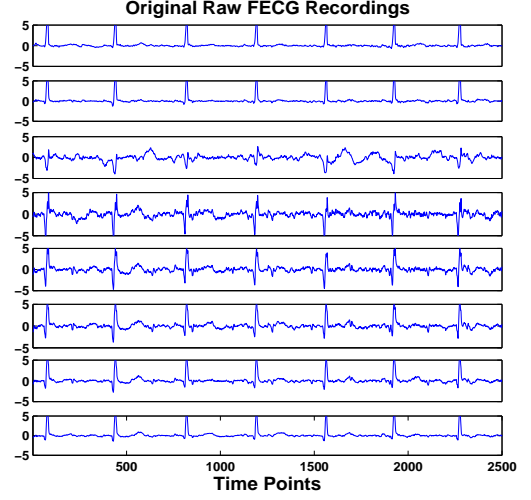


Fig. 8. The original 8-channel abdominal recordings. Fetal cardiac activity is hardly visible in these recordings. Again, each channel recording was normalized to have unit variance for BSS/ICA algorithms.

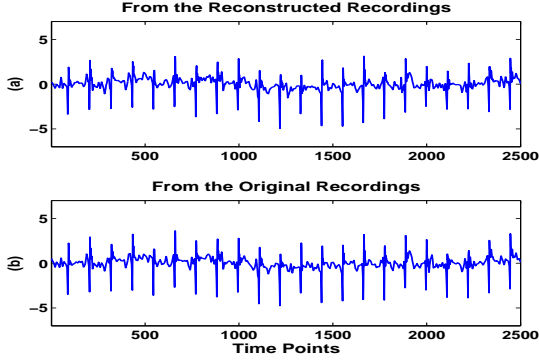


Fig. 7. The extracted FECG from the reconstructed recordings (a) and from the original recordings (b).

### B. FECG Data 2: FECG is Almost Invisible

Now we choose another FECG dataset to test BSBL-BO. In this set of recordings the FECG is almost invisible, so the dataset is more difficult for CS algorithms; any small distortions in the reconstruction may result in the failure of BSS/ICA to extract the FECG. The dataset comes from the Open-Source Electrophysiological Toolbox [38], which consists of eight abdominal recordings of 246 seconds. The original sampling frequency is 1000 Hz. The recordings have passed an analog bandpass filter with a passband of 0.05-100 Hz. In our experiment we downsampled the data to 500 Hz, since in WBAN-based telemonitoring the sampling frequency rarely exceeds 500 Hz. And we only select a subset of recordings of 20 seconds for illustration. Figure 8 shows the recordings of the first 5 seconds.

As in the previous experiment, we used the same sensing matrix  $\Phi$  to compress the recordings and then used CS algorithms to reconstruct them. Again, all the compared algorithms failed to reconstruct the recordings. To save space we do not display their results. Using the same block partition as in the previous experiment, BSBL-BO successfully reconstructed

these recordings (results are not shown here). Then we applied another ICA algorithm, the FastICA algorithm [39], to the reconstructed recordings by BSBL-BO. That we use another BSS/ICA algorithm is to show that the performance evaluation of BSBL-BO is independent of specific BSS/ICA algorithms. Three independent components (ICs) with clear physiological meanings were extracted by FastICA. Two of them were the components of the MECG and the third was the FECG (Fig.9). Then we applied FastICA to the original recordings, also obtaining three ICs (Fig.10). Comparing the results with those in Fig.9, we do not see any distortions. In fact, the correlation between Fig.9 (a) and Fig.10 (a), between Fig.9 (b) and Fig.10 (b), and between Fig.9 (c) and Fig.10 (c) is 0.987, 0.999, 0.974, respectively.

A more strict performance evaluation method is to see if all the ICs obtained by FastICA from the reconstructed recordings are the same as the ones obtained from the original recordings. It is known that raw FECG recordings can be modeled as an ICA mixture model. If distortions in the reconstructed raw FECG recordings are large enough, then the ICA mixing structure will be destroyed. Consequently, all the extracted ICs by FastICA from the reconstructed raw FECG recordings will not be the same as the ICs from the original raw FECG recordings. Figure 11(a) shows all the ICs obtained by FastICA from the reconstructed raw FECG recordings by BSBL-BO, and Figure 11(b) shows all the ICs obtained from the original FECG recordings. Clearly, the ICs in both subfigures are almost the same, confirming that BSBL-BO did not cause large distortions in the reconstructed raw FECG recordings.

### C. Comparison Between BSBL-BO and CS Algorithms In the Wavelet Domain

To reconstruct less-sparse signals, a conventional approach in the CS field is to adopt the model (2). The approach is first reconstructing  $\theta$  using the received data  $y$  and the known matrix  $\Phi\Psi$ , and then calculating  $x$  by  $x = \Psi\theta$ . The

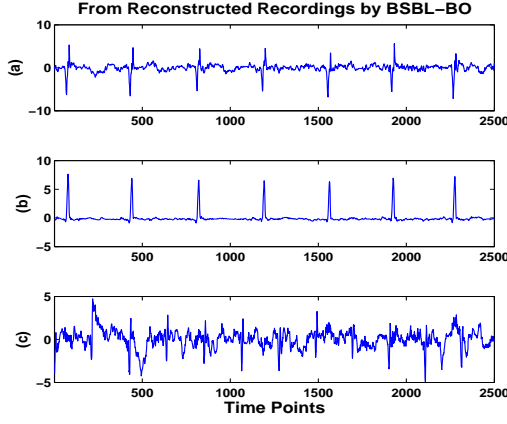


Fig. 9. The extracted MEG and FECG from the reconstructed recordings. (a) and (b) were two independent components of the MEG. (c) was the FECG.

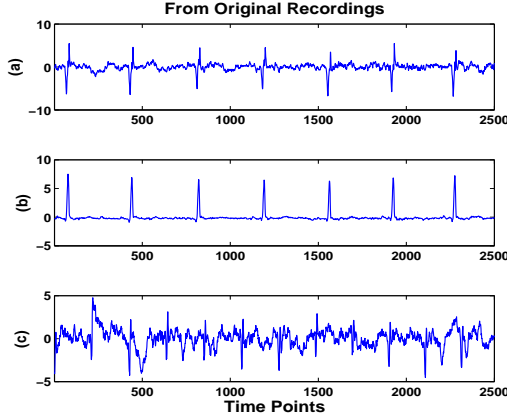


Fig. 10. The extracted MEG and FECG from the original recordings. (a) and (b) were two independent components of the MEG. (c) was the FECG.

dictionary matrix  $\Psi$  is often a wavelet transform matrix. In the following experiment we applied the previous CS algorithms using this approach. Since in [15] it is shown that Daubechies 4 wavelet can yield the sparsest representation of ECG, we set the dictionary matrix  $\Psi$  to be a Daubechies 4 wavelet transform matrix of the size  $256 \times 256$ . The sensing matrix  $\Phi$  was a  $128 \times 256$  sparse binary matrix with each column consisting of 15 entries of 1s. The dataset was the one used in Section III-B. We selected the recordings of the first 12.8 seconds to test algorithms, but here we only display results of the first 5 seconds for visualization.

First, we examined the sparsity of wavelet coefficients of a segment. Figure 12(a) shows the waveform of the segment and Figure 12(b) shows its wavelet coefficients. Clearly, only few wavelet coefficients have large amplitudes, while the majority of coefficients have small amplitudes. The coefficients with large amplitudes correspond to significant characteristics in the segment such as the QRS complexes of the MEG. However, the coefficients with small amplitudes are also important. Very soon we will see that the reconstructed recordings by existing wavelet-based CS algorithms fail to maintain the

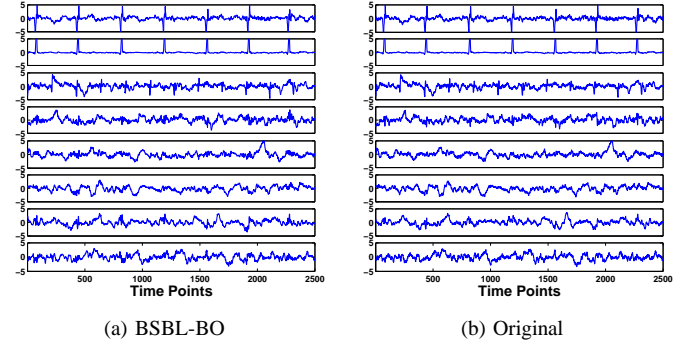


Fig. 11. (a) ICA decomposition from the reconstructed recordings by BSBL-BO. (b) ICA decomposition from the original recordings. In each subfigure the independent components are sorted for better visualization.

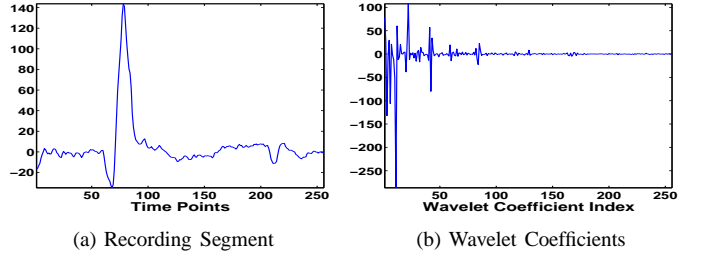


Fig. 12. (a) The segment of the first second of the seventh recording. (b) Daubechies 4 Wavelet coefficients of the segment.

underlying ICA mixing structure because these algorithms fail to reconstruct the wavelet coefficients with small amplitudes.

We applied all the previous CS algorithms on the compressed data  $y$  to reconstruct  $x$  using this wavelet-based approach, and then used FastICA to separate the reconstructed recordings. Again, FastICA successfully extracted the FECG from the recordings reconstructed by BSBL-BO (not shown), but failed to extract the FECG from the recordings reconstructed by other CS algorithms. To save space, we only plot some of the results in Fig.13, which shows the ICA decomposition of the original raw FECG recordings (Fig.13(a)), the ICA decomposition of the recordings reconstructed by BM-MAP-OMP (Fig.13(b)), CluSS-MCMC (Fig.13(c)), and EMBGAMP (Fig.13(d)). Clearly, although the significant characteristics (e.g. the MEG) is maintained in the reconstructed recordings by these CS algorithms, the ICA mixing structure is completely destroyed and no FECG is extracted. In contrast, the ICA decomposition of the recordings reconstructed by BSBL-BO is almost the same as the ICA decomposition of the original recordings. Due to space limit we omit it here.

#### IV. ISSUES ON THE PRACTICAL USE OF BSBL-BO

In previous experiments we used two specific sparse binary sensing matrices and set a specific block partition for BSBL-BO. In this section we will show that the choice of the sparse binary sensing matrix and the block partition is not crucial to the reconstruction performance of BSBL-BO.

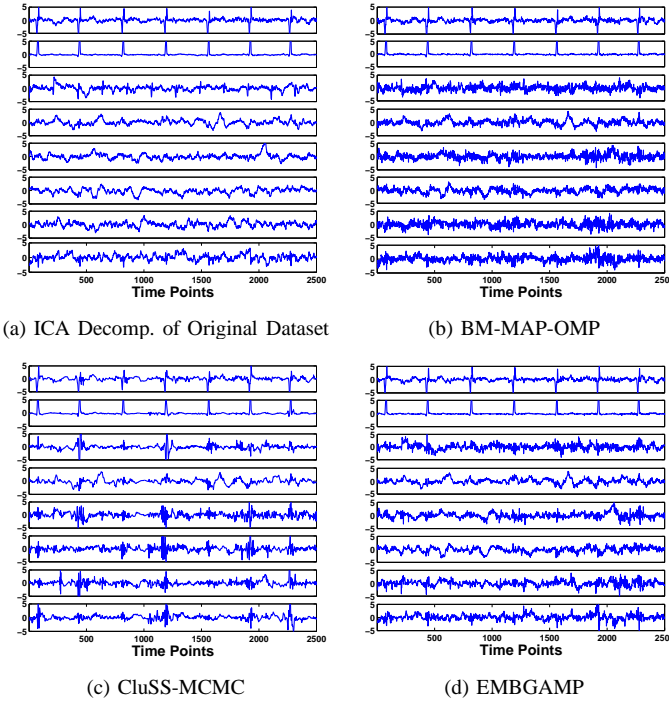


Fig. 13. ICA decomposition from the original recordings (a), from the recordings reconstructed by BM-MAP-OMP (b), from the recordings reconstructed by CluSS-MCMC (c), and from the recordings reconstructed by EMBGAMP (d).

#### A. Effects of the Block Partition

In previous experiments BSBL-BO adopted a specific block partition, namely the location of the first entry of each block was 1, 26, 51,  $\dots$ , 226 (step by 25), respectively. A natural question is, is this block partition related to the block structure of FECGs and MECGs? Particularly, is this block partition designed such that the locations of QRS complexes of FECGs and MECGs are consistent with some of these blocks' locations? In fact, the answer is no. One can notice that in our experiments the block partition was the same for all the recording segments, while in each segment the locations of QRS complexes of FECGs and MECGs were different.

In all the previous experiments we used a fixed block size ( $d = 25$ ). Another question is, whether the block size  $d$  affects the reconstruction quality and thus affects the extraction quality of BSS/ICA? To see this, we carried out the following experiments.

We used the same dataset shown in Fig. 2. The block partition was designed as follows: the location of the first entry of each block was 1,  $1 + d$ ,  $1 + 2d$ ,  $\dots$ , where the block size  $d$  ranged from 5 to 40. The sensing matrix was the one used in Section III-A. For each different  $d$ , we calculated the correlation between the FECG extracted from the reconstructed recordings and the one extracted from the original recordings (the BSS algorithm is the eigBSE algorithm used in Section III-A).

The results are shown in Fig. 14, from which we can see that the extraction quality is high (the correlation is above 0.9) for a large range of  $d$ . In fact, when  $d$  chose values from 6 to

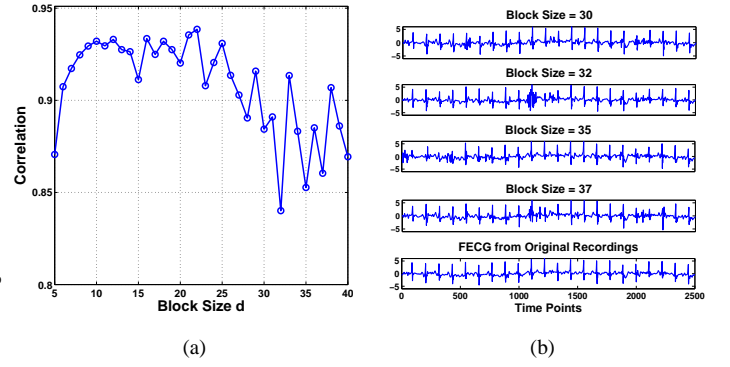


Fig. 14. Effect of the block size  $d$  on the final extraction quality of FECGs when the sensing matrix was of the size  $125 \times 250$  (the dataset is shown in Fig. 2). (a) The correlation between the extracted FECG from the reconstructed recordings and the extracted one from the original recordings when  $d$  ranged from 5 to 40. (b) The extracted FECG from the reconstructed recordings when  $d$  was 30, 32, 35, 37, respectively, compared with the extracted one from the original recordings.

30, the quality is satisfied. Figure 14 (b) gives some extracted FECGs when  $d$  was 30, 32, 35, and 37, respectively. Although the extraction results corresponding to  $d = 32, 35, 37$  are not the best, the quality may be still acceptable. For example, in the extracted FECG corresponding  $d = 32$ , there are only some distortions occurring from the 1100<sup>th</sup> to the 1300<sup>th</sup> time point.

#### B. Effects of the Sensing Matrix Size

The sparse binary matrix  $\Phi$  used in most experiment was of the size  $125 \times 250$ . One may ask another question: is the performance of BSBL-BO sensitive to the size of the sensing matrix? To answer this, we used a large sparse binary matrix whose size was  $250 \times 500$ . Its each column had 28 entries of 1 with random locations. Then we repeated the above experiment with  $d$  ranging from 5 to 40. The results are shown in Figure 15. Compared to the previous experiment results (with the sensing matrix of the size  $125 \times 250$ ), now the extraction quality maintains high quality for a much broader range of  $d$ .

#### C. Effect of Compression Ratio

Now we examine the effects of compression ratio (CR) on the quality of extracted FECGs from reconstructed recordings. Here the compression ratio is defined as

$$CR = \frac{N - M}{N} \times 100 \quad (6)$$

where  $N$  is the length of the original signal and  $M$  is the length of the compressed signal.

We used the dataset shown in Figure 2. The sparse binary sensing matrix was of the size  $M \times N$  where  $N$  was fixed to be 250 while  $M$  varied from 70 to 200. For each value of  $M$ , we took 10 trials. In each trial, the sensing matrix was randomly generated, but its each column always contained 15 entries of 1. After the whole dataset was compressed using the sensing matrix, we used BSBL-BO to reconstruct the recordings, and then extracted a clean FECG from the



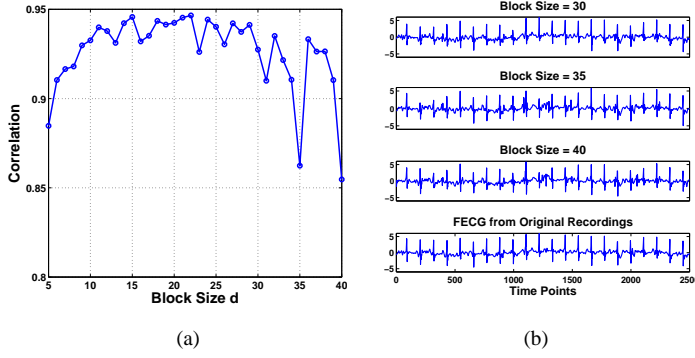


Fig. 15. Effect of the block size  $d$  on the final extraction quality of FECGs when the sensing matrix was of the size  $250 \times 500$  (the dataset is shown in Fig. 2). (a) The correlation between the extracted FECG from the reconstructed recordings and the extracted one from the original recordings when  $d$  ranged from 5 to 40. (b) The extracted FECG from the reconstructed recordings when  $d$  was 30, 35, 40, respectively, compared with the extracted one from the original recordings.

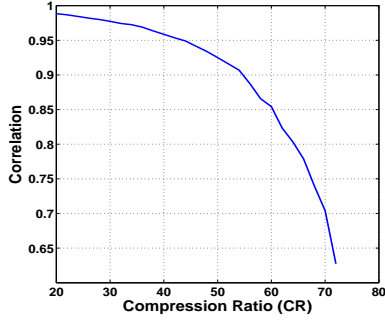


Fig. 16. The effect of the compression ratio on the quality of extracted FECGs from reconstructed recordings (measured by correlation).

reconstructed recordings using the eigBSE algorithm. The extraction quality was measured by its correlation to the FECG extracted from the original recordings. The results averaged over the 10 trials are shown in Figure 16. Note that in previous experiments we have seen when the correlation is higher than 0.85, the extraction quality is acceptable for clinic diagnosis. So the results in Figure 16 indicate that satisfying quality can be achieved when CR does not exceed 60.

## V. DISCUSSIONS

The reconstruction of a raw FECG recording can be cast as a block sparse model with unknown block partition and unknown signal noise in a noiseless environment. To estimate and exploit the unknown block structure, our algorithm is based on a very simple and even counter-intuitive strategy. That is, *the pre-defined block partition is not required to be consistent with the true block structure of the FECG recording*. This strategy is completely different from the strategies used by other CS algorithms to deal with unknown block structure. The successes of our algorithm using this counter-intuitive strategy rely on the powerful ability of the SBL methodology. Theoretical explanation to this empirical phenomenon is an important topic in the future.

Admittedly, the performance of our algorithm is affected by the block size in the block partition. However, this does not

limit its application to wireless FECG telemonitoring. First, we have shown its performance is not sensitive to the block size; a wide range of the block size can lead to satisfying results. Second, the inherent structure of both MEG and FECG does not change too much from case to case, and thus we have enough a priori knowledge to select a suitable block size. Besides, since the reconstruction is operated by software in remote terminals, it is convenient to provide choices for FECG diagnosticians to tune the block size in real-time telemonitoring.

Due to the energy constraint of WBANs as discussed in Section I, the reconstruction of raw FECG recordings requires CS algorithms to have the ability to reconstruct less-sparse signals. Based on our knowledge, the BSBL-BO algorithm is the only one that can directly reconstruct such less-sparse signals and can be used in FECG telemonitoring<sup>4</sup>. Its ability to exploit intra-block correlation is also helpful to reconstruct these structured recordings. Note that it is the first time that the ability of BSBL-BO to reconstruct less-sparse structured signals is revealed and verified by experiments on real-world datasets.

In this work we only focus on the algorithm aspect of wireless FECG telemonitoring. We do not consider system design and compare our algorithm with other conventional methods especially wavelet compression algorithms. The two topics are parts of our future work. However, the previous work by Mamaghanian et al. [11] paves a way for us. Note that essentially the difference between our work and the work by Mamaghanian et al. is the decoding side (i.e. the reconstruction by CS algorithms), which is implemented in software in remote terminals; in the encoding side both work adopted a similar sparse binary sensing matrix. Therefore the advantages of our algorithm in energy consumption and sensor life-time over the wavelet compression algorithms are clear as well. In addition, the entries of our sensing matrices are either zero or one, and the overwhelming majority of entries are zero. This greatly facilitates hardware design and cuts down device cost.

Also, we do not study the design of the sparse binary sensing matrices. Our choice on the sensing matrix is based on the result in [11]. However, it is possible to design a specific sparse binary sensing matrix which leads to higher reconstruction performance or lower algorithmic complexity [40]. Other practical issues such as quantization [41] also have to be studied.

## VI. CONCLUSIONS

Fetal ECG telemonitoring via wireless body-area networks with low-power constraint is a challenge for CS algorithms. In this work we showed that the block sparse Bayesian learning framework [16], [17] can be successfully employed in this task. Its success relies on two unique abilities; one is the ability to reconstruct less-sparse structured signals, and the other is the ability to explore and exploit the unknown structure

<sup>4</sup>There are other two algorithms derived from the bSBL framework, called BSBL-EM and BSBL- $\ell_1$  [16], respectively. However, BSBL-EM is too slow while BSBL- $\ell_1$  has poorer performance in reconstructing FECG recordings, and thus both may not be suitable for FECG telemonitoring.

information of signals to improve performance. Although we focus on the wireless FECG telemonitoring, our algorithm can be used to many other e-Health applications, such as telemonitoring of adult ECG, and wireless electroencephalogram [42].

## REFERENCES

- [1] J. Smith Jr, "Fetal health assessment using prenatal diagnostic techniques," *Current Opinion in Obstetrics and Gynecology*, vol. 20, no. 2, p. 152, 2008.
- [2] M. Hasan, M. Reaz, M. Ibrahimy, M. Hussain, and J. Uddin, "Detection and processing techniques of fecg signal for fetal monitoring," *Biological procedures online*, vol. 11, no. 1, pp. 263–295, 2009.
- [3] R. Sameni, M. Shamsollahi, C. Jutten, and G. Clifford, "A nonlinear bayesian filtering framework for ecg denoising," *IEEE Transactions on Biomedical Engineering*, vol. 54, no. 12, pp. 2172–2185, 2007.
- [4] P. Addison, "Wavelet transforms and the ECG: a review," *Physiological measurement*, vol. 26, p. R155, 2005.
- [5] L. De Lathauwer, B. De Moor, and J. Vandewalle, "Fetal electrocardiogram extraction by blind source subspace separation," *IEEE Transactions on Biomedical Engineering*, vol. 47, no. 5, pp. 567–572, 2000.
- [6] R. Sameni and G. Clifford, "A review of fetal ecg signal processing; issues and promising directions," *The open pacing, electrophysiology & therapy journal*, vol. 3, p. 4, 2010.
- [7] *Special Issue on Cyber-Physical Systems, Proceedings of the IEEE*, 2012, vol. 100, no. 1.
- [8] H. Cao, V. Leung, C. Chow, and H. Chan, "Enabling technologies for wireless body area networks: A survey and outlook," *IEEE Communications Magazine*, vol. 47, no. 12, pp. 84–93, 2009.
- [9] A. Milenkovic, C. Otto, and E. Jovanov, "Wireless sensor networks for personal health monitoring: Issues and an implementation," *Computer communications*, vol. 29, no. 13–14, pp. 2521–2533, 2006.
- [10] B. Calhoun, J. Lach, J. Stankovic, D. Wentzloff, K. Whitehouse, A. Barth, J. Brown, Q. Li, S. Oh, N. Roberts, et al., "Body sensor networks: A holistic approach from silicon to users," *Proceedings of the IEEE*, vol. 100, no. 1, pp. 91–106, 2012.
- [11] H. Mamaghanian, N. Khaled, D. Atienza, and P. Vanderghenst, "Compressed sensing for real-time energy-efficient ECG compression on wireless body sensor nodes," *IEEE Transactions on Biomedical Engineering*, vol. 58, no. 9, pp. 2456–2466, 2011.
- [12] D. Donoho, "Compressed sensing," *Information Theory, IEEE Transactions on*, vol. 52, no. 4, pp. 1289–1306, 2006.
- [13] R. G. Baraniuk, "Compressive sensing," *IEEE Signal Processing Magazine*, vol. 24, no. 4, pp. 118–121, 2007.
- [14] E. Candes, J. Romberg, and T. Tao, "Stable signal recovery from incomplete and inaccurate measurements," *Communications on pure and applied mathematics*, vol. 59, no. 8, pp. 1207–1223, 2006.
- [15] C. Eduardo, P. Octavian Adrian, S. Pedro, et al., "Implementation of compressed sensing in telecardiology sensor networks," *International Journal of Telemedicine and Applications*, vol. 2010, 2010.
- [16] Z. Zhang and B. Rao, "Extension of SBL algorithms for the recovery of block sparse signals with intra-block correlation," *IEEE Trans. on Signal Processing (submitted)*, 2012. [Online]. Available: arXiv:1201.0862
- [17] —, "Sparse signal recovery with temporally correlated source vectors using sparse Bayesian learning," *IEEE Journal of Selected Topics in Signal Processing*, vol. 5, no. 5, pp. 912–926, 2011.
- [18] —, "Recovery of block sparse signals using the framework of block sparse Bayesian learning," in *2012 IEEE International Conference on Acoustics, Speech and Signal Processing (ICASSP)*, 2012.
- [19] —, "Exploiting correlation in sparse signal recovery problems: Multiple measurement vectors, block sparsity, and time-varying sparsity," in *ICML 2011 Workshop on Structured Sparsity: Learning and Inference*, 2011. [Online]. Available: http://arxiv.org/pdf/1105.0725
- [20] J. Wan, Z. Zhang, J. Yan, T. Li, B. D. Rao, and et al, "Sparse Bayesian multi-task learning for predicting cognitive outcomes from neuroimaging measures in Alzheimers disease," in *CVPR 2012*.
- [21] E. Arias-Castro and Y. Eldar, "Noise folding in compressed sensing," *IEEE Signal Processing Letters*, vol. 18, no. 4, pp. 478 – 481, 2011.
- [22] R. G. Baraniuk, V. Cevher, M. F. Duarte, and C. Hegde, "Model-based compressive sensing," *IEEE Trans. on Information Theory*, vol. 56, no. 4, pp. 1982–2001, 2010.
- [23] Y. C. Eldar, P. Kuppinger, and H. Bolcskei, "Block-sparse signals: uncertainty relations and efficient recovery," *IEEE Trans. on Signal Processing*, vol. 58, no. 6, pp. 3042–3054, 2010.
- [24] J. Huang, T. Zhang, and D. Metaxas, "Learning with structured sparsity," in *Proceedings of the 26th Annual International Conference on Machine Learning*, 2009, pp. 417–424.
- [25] L. Yu, H. Sun, J. P. Barbot, and G. Zheng, "Bayesian compressive sensing for cluster structured sparse signals," *Signal Processing*, vol. 92, no. 1, pp. 259–269, 2012.
- [26] T. Faktor, Y. Eldar, and M. Elad, "Exploiting statistical dependencies in sparse representations for signal recovery," *Arxiv preprint arXiv:1010.5734*, 2010.
- [27] Z. Zhang and B. Rao, "Clarify some issues on the sparse Bayesian learning for sparse signal recovery," *Technical Report, University of California, San Diego*, Sep. 2011. [Online]. Available: http://dsp.ucsd.edu/~zhilin/papers/clarify.pdf
- [28] M. E. Tipping, "Sparse Bayesian learning and the relevance vector machine," *J. of Mach. Learn. Res.*, vol. 1, pp. 211–244, 2001.
- [29] Z. Wang and A. Bovik, "Mean squared error: Love it or leave it? a new look at signal fidelity measures," *IEEE Signal Processing Magazine*, vol. 26, no. 1, pp. 98–117, 2009.
- [30] B. D. Moor, "DaSy: Database for the identification of systems," November 2011. [Online]. Available: http://www.esat.kuleuven.ac.be/sista/daisy
- [31] E. Allstot, A. Chen, A. Dixon, D. Gangopadhyay, and D. Allstot, "Compressive sampling of ECG bio-signals: Quantization noise and sparsity considerations," in *2010 IEEE Conference on Biomedical Circuits and Systems (BioCAS)*, 2010, pp. 41–44.
- [32] L. Polania, R. Carrillo, M. Blanco-Velasco, and K. Barner, "Compressed sensing based method for ECG compression," in *2011 IEEE International Conference on Acoustics, Speech and Signal Processing (ICASSP)*, 2011, pp. 761–764.
- [33] D. Needell and J. A. Tropp, "CoSaMP: Iterative signal recovery from incomplete and inaccurate samples," *Applied and Computational Harmonic Analysis*, vol. 26, no. 3, pp. 301–321, 2009.
- [34] H. Zou and T. Hastie, "Regularization and variable selection via the elastic net," *Journal of the Royal Statistical Society: Series B (Statistical Methodology)*, vol. 67, no. 2, pp. 301–320, 2005.
- [35] H. Mohimani, M. Babaie-Zadeh, and C. Jutten, "A fast approach for overcomplete sparse decomposition based on smoothed l0 norm," *IEEE Trans. on Signal Processing*, vol. 57, no. 1, pp. 289–301, 2009.
- [36] J. Vila and P. Schniter, "Expectation-maximization bernoulli-gaussian approximate message passing," in *Proc. Asilomar Conf. on Signals, Systems, and Computers*, 2011.
- [37] Z.-L. Zhang and Z. Yi, "Robust extraction of specific signals with temporal structure," *Neurocomputing*, vol. 69, no. 7–9, pp. 888–893, 2006.
- [38] R. Sameni, "OSET: The open-source electrophysiological toolbox," January 2012. [Online]. Available: http://www.oset.ir/
- [39] A. Hyvarinen, "Fast and robust fixed-point algorithms for independent component analysis," *IEEE Transactions on Neural Networks*, vol. 10, no. 3, pp. 626–634, 1999.
- [40] A. Gilbert and P. Indyk, "Sparse recovery using sparse matrices," *Proceedings of the IEEE*, vol. 98, no. 6, pp. 937–947, 2010.
- [41] J. Laska, P. Boufounos, M. Davenport, and R. Baraniuk, "Democracy in action: Quantization, saturation, and compressive sensing," *Applied and Computational Harmonic Analysis*, vol. 31, pp. 429–443, 2011.
- [42] C. Lin, L. Ko, J. Chiou, J. Duann, R. Huang, S. Liang, T. Chiu, and T. Jung, "Noninvasive neural prostheses using mobile and wireless EEG," *Proceedings of the IEEE*, vol. 96, no. 7, pp. 1167–1183, 2008.